Biogeosciences Discuss., 12, 2381–2427, 2015
www.biogeosciences-discuss.net/12/2381/2015/
doi:10.5194/bgd-12-2381-2015

Biogeosciences Discussions
Open Access

Mesozooplankton structure and functioning during the onset of the Kerguelen phytoplankton bloom during the Keops2 survey

F. Carlotti[1], M.-P. Jouandet[1], A. Nowaczyk[1], M. Harmelin-Vivien[1], D. Lefèvre[1], G. Guillou[2], Y. Zhu[1,3], and M. Zhou[1,3]

[1]Aix Marseille Université, CNRS/INSU, Université de Toulon, IRD, Mediterranean Institute of Oceanography (MIO), UM110, 13288, Marseille, France
[2]Littoral Environnement et Sociétés, UMR7266 CNRS-Université de La Rochelle, 2 Rue Olympe de Gouges, 17000 La Rochelle, France
[3]University of Massachusetts Boston, Boston, MA 02125, USA

Received: 28 November 2014 – Accepted: 5 December 2014 – Published: 4 February 2015

Correspondence to: F. Carlotti (francois.carlotti@univ-amu.fr)

Published by Copernicus Publications on behalf of the European Geosciences Union.

Abstract

This study presents results on the zooplankton response to the early phase of the northeastern Kerguelen bloom during the KEOPS2 survey (15 October–20 November 2011). The campaign combined a large coverage of the eastern part of the shelf and the adjacent oceanic regions with 2 quasi-perpendicular transects oriented south to north (between 49°08′ and 46°50′ S) and west to east (between 69°50′ and 74°60′ E) aiming to document the spatial extension of the bloom and its coastal-off shore gradient, and a pseudo-lagrangian survey located in a complex recirculation zone in a stationary meander of the Polar front nearly centered at the crossing of the 2 initial transects. In addition, 8 stations were performed for 24 h observations, distributed in key areas and some of them common with the KEOPS1 cruise (January–February 2005). The mesozooplankton biomass stocks observed at the beginning of the KEOPS2 cruise were around 2 g C m^{-2} both above the plateau and in oceanic waters. Zooplankton biomasses in oceanic waters were maintained in average below 2 g C m^{-2} over the study period, except for one station in the Polar Front Zone (FL), whereas zooplankton biomasses were around 4 g C m^{-2} on the plateau at the end of the cruise. Taxonomic composition and stable isotope ratios of size-fractionated zooplankton indicated the strong domination of herbivores. The most remarkable feature during the sampling period was the stronger increase in the integrated 0–250 m abundances in the oceanic waters (25×10^3 to 160×10^3 ind m^{-2}) than on the plateau (25×10^3 to 90×10^3 ind m^{-2}). The size structure and taxonomic distributions revealed a cumulative contribution of various larval stages of dominant copepods and euphausiids particularly in the oceanic waters, with clearly identifiable stages of progress during the Lagrangian survey. These different results during KEOPS2 suggested that the zooplankton community was able to respond to the growing phytoplankton blooms earlier on the plateau than in the oceanic waters. The reproduction and early stage development of dominant species were sustained by mesoscale-related initial ephemeral blooms in oceanic waters but individual growth was still food-limited and zooplankton biomass stagnated.

BGD
12, 2381–2427, 2015

On the contrary, zooplankton abundances and biomasses on the shelf were both in a growing phase, with slightly different rates, due to sub-optimal conditions of growth and reproduction conditions. Combined with the KEOPS1, the present results deliver a consistent understanding of the spring changes in zooplankton abundance and biomass in the Kerguelen area.

1 Introduction

In the path of the eastward flow of Antarctic Circumpolar Current, the Kerguelen Plateau oriented along the 70° E meridian forms a large north-west/south-east topographic barrier, and the meandering course of the Polar Front (PF) around the Kerguelen Islands has important implications for the productivity in the eastern area of the island. During the winter-spring period, flows along the PF above the plateau south of the Kerguelen Islands induce entrainment and mixing of Fe enriched shelf waters from plateau sediments in the oceanic upper layer in the eastern area of Kerguelen. The PF current is assumed to drive relatively high phytoplankton bloom concentrations (Blain et al., 2007) in contrast with the generally high-nutrient, low-chlorophyll (HNLC) surface waters of the Southern Ocean. This eastern part of the Kerguelen Plateau sustains the most important local foraging areas for land-based marine predators (birds, penguins, seals, and elephant seals) and for whales (Hindell et al., 2011; Blain et al., 2013), showing that secondary production, such as zooplankton and fish required to meet this demand, should quickly match and transfer the new primary production.

During the KEOPS1 cruise (The KErguelen Ocean and Plateau compared Study), the origin and fate of the elevated phytoplankton biomass in naturally iron-fertilized waters over the Kerguelen plateau (South-East area) was examined (Blain et al., 2008). Throughout the decline phase (January-February 2005) of the natural long-term bloom (> 3 months), the mesozooplankton populations were already well established, with no significant spatial and temporal changes in biomass and species composition (Carlotti et al., 2008). The potential role of the mesozooplankton, mainly copepods, in driving

BGD
12, 2381–2427, 2015

the particle flux by grazing and faecal pellet production was highlighted during the KEOPS1 by observations in polyacrylamide gels placed in free-drifting sediment traps at two sites, over the central plateau and at its periphery (Ebersbach and Trull, 2008).

In contrast, the present KEOPS2 cruise aimed to complement the findings of KEOPS1 above the Kerguelen plateau, and gained new insights on the biogeochemistry and ecosystem response to iron fertilization by examining its structure and dynamics in the early phase of the bloom (October-November 2011) and extending the study area to the oceanic deep waters north-east of the Kerguelen Islands.

The eastern side of the Kerguelen region is as well marked by an increase of the mixed layer integrated chlorophyll from October to December (Blain et al., 2013), due to a phytoplankton bloom, initially dominated by diatoms of high growth rates (Quéguiner, 2013). Zooplankton development in connection to spring bloom has not been yet documented in this oceanic region. Zooplankton distributions observed by Semelkina (1993) during the SKALP cruises around the Kerguelen Islands (46–52° S, 64–73° E) from February 1997 to February 1998 showed a change in biomass (4-fold higher) from winter (July-August) to mid-summer (February), but do not describe this early spring period. Zooplankton biomasses observed by Carlotti et al. (2008) in summer (January-February 2005) in the eastern sector of the Kerguelen fluctuated around 10.6 g C m^{-2} above the plateau (their station A3) and were around or below 5 g C m^{-2} in oceanic waters (excepted their station A9), showing an enhanced secondary production in naturally iron-fertilized waters. Despite the particular environmental conditions above the plateau, it is worthwhile to note that the seasonal zooplankton abundances recorded from February 1992 to January 1995 at the KERFIX station, located around 60 miles southwest of the Kerguelen Islands in 1700 m of water, show a major increase in copepods densities from September to January (Razouls et al., 1998).

Descriptions of seasonal variations of mesozooplankton standing stocks in Antarctica oceanic regions are scarce. The implementation of Southern Ocean CPR surveys delivers a consistent information about the seasonal succession of zooplanktonic communities in the Southern Ocean south of Australia (Hosie et al., 2003; Hunt and Hosie,

BGD
12, 2381–2427, 2015

2006a, b). In the polar front zone, a relative strong increase of zooplankton abundance occurs in spring, from October-November (see Hosie et al., 2003, their Fig. 3) mainly due to changes in densities of all common taxa from average winter levels still maintained until October (Hunt and Hosie, 2006b). The largest copepods of the region (*Rhincalanus gigas*, *Calanoides acutus*, *Ctenocalanus citer*) are seasonal migrators which arrive in the surface layer from winter diapause depths when Chl *a* concentrations increase (October-November). Overwintering females may spawn reserves even before the full bloom, whereas overwintering stages other than adult stages resume their growth in surface water up to mature adults which produce new cohorts during the full bloom period (Atkinson, 1998; Hunt and Hosie, 2006b). Other smaller species (*Calanus similimus*, *Oithona* sp., ...) resume their population development from survivors from the previous year and start reproduction earlier in spring (Atkinson, 1998).

The main objective of the present study was to investigate the density, diversity and biomass of zooplankton during this early bloom phase at all sampled stations during the KEOPS2 cruise, and its responses to primary production in contrasted environments differently impacted by iron availability and mesoscale activity.

2 Material and methods

2.1 Study site and sampling strategy

The KEOPS2 survey was performed east of the Kerguelen Islands in the Indian sector of the Southern Ocean, on board R/V *Marion Dufresne*, between the 15 October and the 20 November 2011. It first consisted in 2 quasi-perpendicular transects oriented south to north (between 49°08′ S and 46°50′ S) and west to east (between 69°50′ E and 74°60′ E) aim to document the spatial extension of the bloom and its coastal-off shore gradient. During these transects, zooplankton samples were collected at 10 stations along a North–South transect (TNS) and at 8 stations along an East–West transect (TEW) (Fig. 1). The East–West transect crossed the Polar front twice. Firstly

BGD
12, 2381–2427, 2015

between TEW3 and TEW4 where the southern branch of the PF flowed northwards along the shelf-break, and secondly between TEW6 and TEW7, where the PF was directed southwards after a semicircle trajectory maintaining a large stationary meander in this area. The most western stations were located over the inner (TEW1) and outer (TEW2) parts of the Kerguelen shelf. The most eastern stations (TEW7 and TEW8) were situated in Subantarctic Mode Water whereas the central section (TEW4 to TEW6) within the stationary meander was bathed by mixed Antarctic surface water (Farias et al., 2015). In addition, 8 long-term stations were performed for 24 h process studies during which zooplankton samples were taken twice a day, at day and night time (Fig. 1): a HNLC reference station (R-2) located outside the bloom in deep waters south-west of Kerguelen Islands, the Kerguelen Plateau central bloom reference station of KEOPS1 (A3) also visited two times during KEOPS2, a productive open ocean station (FL) influenced by warmer sub-antarctic surface waters, located north of the Polar Front, a productive station (E4W) located in the plume of chlorophyll observed down- stream of the plateau and close to the jet induced by the PF, and 5 stations (E1, E2, E3, E4E and E5) constituting a pseudo-lagrangian survey located in a complex recirculation zone in a stationary meander of the Polar front characterized by strong mesoscale activity, nearly centered at the crossing of the 2 initial transects (Park et al., 2014; Zhou et al., 2014). Real time satellite images (chlorophyll and altimetry) in combination with trajectories of 50 drifters released during the first part of the cruise were used to carefully decide the positions of these latter stations (d'Ovidio et al., 2015).

The oceanographic circulation patters pertinent to the KEOPS2 study are presented in Park et al. (2014). How the macro- and micro-nutrient availability linked to the physical processes that initiates and sustains phytoplankton growth and primary production is presented in companion papers: Lasbleiz et al. (2014), Trull et al. (2014), Blain et al. (2014), Closset et al. (2014). The fate of the primary production both through heterotrophy and sinking is analyzed in other companion papers: Christaki et al. (2014), Jacquet et al. (2014), Jouandet et al. (2014), Laurenceau et al. (2014). Complemen-

BGD
12, 2381–2427, 2015

tary information on satellite-image-derived primary production has been supplied by D'Ovidio (personal communication, 2011).

2.2 Mesozooplankton sampling

Zooplankton collection were conducted at 27 stations with a double Bongo nets (60 cm mouth diameter) fitted with 330 mm mesh sizes mounted with filtering cod ends. Hauls were done from 250 m depth to the surface at 0.5 ms^{-1}. The 10 stations of the North–South transect (TNS) and the 8 stations of the East–West transect (TEW) were sampled once each. During the long-term stations (A3 visited two times, R, F, and the set of the stations E) zooplankton samples were taken twice a day, at day and night time.

The content of one of the two nets was preserved in 4 % borax-buffered formalin seawater for further laboratory study of zooplankton community structure (taxonomy, abundance and size structure) and biomass estimates from organism biovolume (see below). The cod-end content of the second net was kept fresh and split into two parts with a Motoda box (Motoda, 1959). The first part was processed immediately for dry weight measurements. The second half of the sample was fractionated immediately onboard using a filtration column with six sieves with 80, 200, 300, 500, 1000 and 2000 µm meshes for further isotopes analysis (see below). The two first size classes (80–200 µm and 200–300 µm) include small organisms caught by the net because of clogging. For the largest size class (> 2000 µm), large organisms such as salps and euphausiids were separated in additional containers. Then, the samples were placed in small containers and immediately deep-frozen (−80 °C).

2.3 Abundances and biomasses using the Zooscan

Net tow samples from all stations were processed using ZOOSCAN (www.zooscan.com) to determine the size structure of the zooplankton communities. ZOOSCAN has been recently used to study zooplankton community in various areas and has been validated by comparisons with traditional sampling methods (Grosjean et al., 2004;

BGD
12, 2381–2427, 2015

Schultes and Lopes, 2009; Gorsky et al., 2010). Our ZOOSCAN setup is similar to the one described by Gorsky et al. (2010), and our sample processing protocol is fully described in Nowaczyk et al. (2011), following Gorsky et al. (2010) recommendations.

After homogenization, each sample was quantitatively split with a Motoda box once back in the laboratory and a fraction of each preserved sample containing a minimum of 1000 particles (in general 1/32 or 1/64 of the whole sample) was placed on the glass plate of the ZOOSCAN. Organisms were carefully separated one by one manually with a wooden spine, in order to avoid overlapping. Each image was then run through ZooProcess plug-in using the image analysis software Image J (Grosjean et al., 2004; Gorsky et al., 2010). Several measurements of each organism were then computerized. Organism size is given by its equivalent circular diameter (ECD) and can then be converted into biovolume, assuming each organism is an ellipsoid (more details in Grosjean et al., 2004). The lowest ECD detectable by this scanning device is 300 µm. To discriminate between aggregates and organisms, we used a training set of about 1000 objects which were selected automatically from 40 different scans. This protocol allows discrimination between aggregates and organisms by building the initial training set of images.

The biovolume (BV, mm^3) was calculated from the organism image areas and morphometric parameters. In order to estimate the biomass of each organism, we used the same conversion as in Carlotti et al. (2008), each measured biovolume (BV, mm^3) of a zooplankton individual was converted into biomass (W, mg DW) using the following relationship:

$\log(W) = 0.865 \log(\mathrm{BV}) - 0.887$ (Riandey et al., 2005).

Carbon content has been assumed to be 50 % of body dry weight.

In this article, the terms ZOOSCAN abundance and ZOOSCAN biomass will designate the values derived from the laboratory ZOOSCAN treatment. The abundance and biomass of organisms were then grouped into four size fractions (< 500, 500–

BGD
12, 2381–2427, 2015

1000, 1000–2000, and > 2000 µm) based on their ECD, and summed to deliver the total abundance and biomass per sample over the 250 upper meters.

The choice of the net tow sampling depth was based on mixed layer depth found at the first station of the cruise, and maintained afterwards. Abundance and biomass values are normalized to the volume of water filtered in situ. ANOVA test (5 % significance level) was used to test differences of abundance and biomass between stations or oceanic areas.

2.4 Taxonomic determination

Very common taxa were counted in subsamples (1/32 or 1/64) and at least 600 individuals were enumerated per subsample. The whole sample was examined for either rare species and/or large organisms (i.e. euphausiids, amphipods). Identification of the copepod community was made down to species level and groups of developmental stage when possible. Species/genus identification was made according to Rose (1933), Tregouboff and Rose (1957) and Razouls et al. (2005–2014). Organisms other than copepods as well as meroplankton were identified down to taxa levels. Identifications were done to genus level for copepods, amphipods, pelagic molluscs, polychaetes, Thaliacea and Cnidarians; and to taxa level for other major holoplanktonic and meroplanktonic groups. To identify which taxonomic groups contribute to the four size fractions defined from the ZOOSCAN measurements (see above), each observed organism was classified as small, medium, large, or very large mesozooplankton which almost corresponded to the four size fractions determined by ZOOSCAN based on ECD (< 500, 500–1000, 1000–2000, and > 2000 µm).

2.5 Biomass measurement

The subsample for bulk biomass measurement was filtered onto pre-weighted and pre-combusted GF/F filter (47 mm) which was quickly rinsed with distilled water and dried in an oven at 60 °C for 3 days onboard. Dry-weight (mg) of 19 samples was calculated

BGD
12, 2381–2427, 2015

from the difference between the final weight and the weight of the filter and biomass (mg DW m^{-2}) was extrapolated from the total volume sampled by the net.

2.6 Stable isotopes analysis

Before being processed, identification of broad taxonomic composition of each sample was performed under a binocular microscope. When possible, main group of organisms in the largest > 2000 µm size-fraction were sorted out and processed separately. Then, zooplankton fractions were freeze-dried and ground into a homogeneous powder. As they may contain carbonates, an acidification step was necessary to remove ^{13}C-enriched carbonates (DeNiro and Epstein, 1978; Søreide et al., 2006). A subsample was acidified with 1 % HCl, rinsed, dried and used for δ^{13}C determination, while the other untreated subsample was used for δ^{15}N analysis. Three replicates were performed on each plankton fraction per sampled station for both δ^{13}C and δ^{15}N. Stable isotope measurements were performed with a continuous-flow isotope-ratio mass spectrometer (Delta V Advantage, Thermo Scientific, Bremmen, Germany) coupled to an elemental analyzer (Flash EA1112 Thermo Scientific, Milan, Italy). Results are expressed in parts per thousand (‰) relative to Vienna Pee Dee Belemnite and atmospheric N_2 for δ^{13}C and δ^{15}N, respectively, according to the equation:

$$\delta X = [(R_{\text{sample}}/R_{\text{standard}}) - 1] \cdot 10^3,$$

where X is ^{13}C or ^{15}N and R is the isotope ratio ^{13}C/^{12}C or ^{15}N/^{14}N, respectively. For both δ^{13}C and δ^{15}N, measurement precision is < 0.1 ‰ (replicate measurements of internal laboratory acetanilide standard). Percentage of organic C and organic N were obtained using the elemental analyzer and were used to calculate the sample C/N ratio.

Lipids are depleted in δ^{13}C relative to proteins and carbohydrates, and variation in lipid content among organisms can introduce considerable bias into carbon stable isotope analyses (Bodin et al., 2007; Post et al., 2007). Like most polar marine organisms

BGD
12, 2381–2427, 2015

(Lee et al., 2006), KEOPS2 zooplankton fractions could present a high lipid content (up to 20 % dry mass, MHV data not shown), reflected by high C/N values. Thus, $\delta^{13}C$ acidified sample values of fractions > 200 µm were corrected according to the formula calculated by Post et al. (2007) for aquatic organisms, using the C/N ratio of each sample:

$$\delta^{13}C_{normalized} = \delta^{13}C_{acidified} - 3.32 + 0.99 \cdot C/N$$

Acidified $\delta^{13}C$ values of the lowest size-fraction (80–200 µm) were not lipid corrected due to their low lipid content (< 5 %, MHV data not shown). The resulting $\delta^{13}C_{normalized}$ provides an estimate of $\delta^{13}C$ corrected for the effects of lipid concentration. Lipid correction calculated by Smyntek et al. (2007) for zooplankton give $\delta^{13}C$ values 0.63 ± 0.01 ‰ lower than by Post et al. (2007). As $\delta^{13}C$ values provided by Trull et al. (2014) were not lipid normalized, acidified $\delta^{13}C$ values for all zooplankton size-fractions were indicated in Table 2, along with lipid normalized $\delta^{13}C$ values, to allow comparisons between the two data series.

2.7 Data analysis

The effect of stations and dates (n = 12) on zooplankton abundance and biomass was tested statistically using one-way ANOVA with the statistical software Statistica v7. The statistical significance was tested at the 95 % confidence level. Community patterns for taxa abundances were explored using the Primer (V6) software package which has been shown to reveal patterns in zooplankton communities (e.g. Clarke and Warwick, 2001; Wishner et al., 2008). Data sets were power transformed (4th root), and the Bray–Curtis dissimilarity index between stations (Bray and Curtis, 1957) was calculated employing all taxonomic categories that contributed at least 1 % to any sample in that dataset. Different groups of zooplankton (BC-Groups) were individualized based on their taxonomic composition. Mean C and N stable isotope values among size-fraction and between day and night within each fraction were compared by one-way ANOVAs

BGD
12, 2381–2427, 2015

followed by Tukey post-hoc tests, after testing for normality by Levene test. The spatial organisation of sites was analysed by hierarchical clustering based on mean $\delta^{13}C$ and $\delta^{15}N$ values using complete linkage and Euclidean distance. Different isotopic groups of stations (IS-Groups) were thus individualized and compared with the station grouping defined by Trull et al. (2014) based on chemometric measurements (T-Groups). T-Group 4, corresponding to coastal stations, was not sampled for stable isotope analysis of zooplankton.

3 Results

3.1 Temporal and spatial variations of zooplankton abundance and biomass

Zooplankton abundances and biomass from ZOOSCAN varied from 14×10^3 to 200×10^3 ind m^{-2} (Fig. 2) and from 0.25 to 4.94 g C m^{-2} (Fig. 3), respectively. Comparisons of abundance (ind m^{-2}) and biomass (g C m^{-2}) between ZOOSCAN-derived data and direct measurements showed that ZOOSCAN-derived data slightly overestimated direct measurements from regression forced through the origin: slope equal to 1.0015 for abundances ($R^2 = 0.75$, $n = 37$, $p < 0.01$) and slope equal to 1.1246 for dry weight ($R^2 = 0.803$, $n = 19$, $p < 0.01$).

Abundance values followed a normal distribution with an average of 73×10^3 ind m^{-2} (SD: 42). ANOVA with main effects (stations and dates) without interaction showed clear effect for dates ($p < 0.05$) but not for stations. All abundance values plotted against dates (Fig. 4a) showed a general increase, and the linear regression ($R^2 = 0.42$, $n = 37$) predicted a ratio of 3.7 between abundances at the beginning and at the end of the survey. Highest abundances (above the regression line on Fig. 4a) were observed for oceanic stations within the PF meander, both for the stations of the two transects (Stations TNS4, 5, 7, 8, and TEW 4, 6, 7, 8, and stations E, except for E4-West). On the contrary, the lowest abundances were found on the East and North of this PF meander, as well as for the first visit in A3. One exception was the station TEW5

BGD
12, 2381–2427, 2015

which presented the lowest abundances whereas near spatial and temporal sampling stations presented much higher abundances. Between the two visits at the station A3 at the beginning and the end of the survey, the total abundances were multiplied by 3.5.

The fraction 500–1000 µm (see Fig. 3) presented the most abundant number of organisms (62.0 % in average percentage), followed by the < 500 µm fraction (18.8 % in average percentage), the 1000–2000 µm fraction (14.2 % in average percentage) and the > 2000 µm fraction (5.0 % in average percentage). The contribution of the smaller size fraction (< 500 µm) increased with time from the beginning to the end of the survey (8.1 % in average), whereas the 500–1000 µm, 1000–2000 µm, and > 2000 µm decreased to 5.0, 0.8 and 2.3 % respectively. However, it was not significant in any of the four regressions due to the variability in size distribution between the stations. In addition, no clear diurnal patterns was observed from the day/night samplings realized at 9 sampling dates

Log-transformed biomass values followed a normal distribution. As for the abundances, ANOVA with main effects (stations and dates) without interaction for biomass values showed an effect for dates ($p < 0.05$) but not for stations. Average biomass was 2.32 g C m^{-2} (SD: 1.33), and the linear regression against time (not significant) predicted a ratio of 1.7 between biomass values at the beginning and the end of the survey (Fig. 4b). However the biomass ratio at the station A3 between the two visits showed an increase of 2.9, whereas the biomass values of the station E (the pseudo-lagrangian survey) showed a slightly decreasing trend (with the exception of E4-En). The fraction > 2000 µm represented the highest biomass of organisms (57.1 % in average percentage), followed by the 1000–2000 µm, 500–1000 µm and < 500 µm fractions with 22.8, 18.2 and 1.9 % in average percentage, respectively (see Fig. 2). Any of the regression between the percentage value and dates presented a significant correlation, and the slopes of the regression were all near to zero for the intermediate size fractions. From the beginning to the end of the survey, the largest size fraction (> 2000 µm) decreased in its contribution to the biomass (−1.5 %), whereas the contribution to the

BGD
12, 2381–2427, 2015

biomass increased with time of 0.1, 0.5 and 0.9 % respectively for the 1000–2000 µm, 500–1000 µm and < 500 µm fractions.

The total zooplankton biomass values presented a significant correlation ($p < 0.01$) with the average chlorophyll concentrations in the 100 upper meters, as well as with the integrated chlorophyll concentrations in the mixed layer depth (Fig. 5). Only the stations TEW1 and TEW2 presented low zooplankton biomass for relative high fluorescence concentrations (> 1 µg Chl *a* L^{-1}, Fig. 5a), but not vs. the integrated Chl *a* biomass in their narrow (< 80 m) mixed layer (Fig. 5b).

3.2 Metazooplankton community composition and distribution

65 taxa were identified from net tows for the 37 stations of this study (Table 1) with 26 genera/species of copepods. Copepods contributed the bulk of the zooplankton community abundance with 78.4 % (SD = 13.13 %) of the counted organisms over the whole area, and copepodites represented a bit more than half of the counted copepods (mean = 52.5 %, SD = 8.2 %). ANOVA with main effects (stations and dates) without interaction showed no effect either for dates or for stations both for the percentage of copepods against the whole zooplankton abundance, and for the percentage of copepodites stages against the total copepods abundance. Nauplii represented an average 2 % of the total abundance, and showed an increasing abundance with time up to 4 %, althought they were undersampled with our net. The copepod communities was dominated by *Ctenocalanus citer*, followed by *Oithona similis* and *O. frigida*, *Metridia lucens*, *Scolecithricella minor*, *Calanus simillimus*, *Paraeuchaeta* spp., *Rhincalanus gigas*, and near coastal area *Drepanopus pectinatus*. Other dominant taxa were the different larval stages of euphausiids (eggs, nauplii, metanauplii, proto et metaozoe), appendicularians (*Oïkopleura* spp., *Fritillaria* spp.), chaetognaths, pteropods (*Limacina retroversa*), amphipods (*Themisto gaudicaudii*, *Hyperia* spp.). Radiolarians and foraminifera were regularly sampled as well. In some stations other taxa occurred in low numbers, such as salps.

BGD
12, 2381–2427, 2015

The distribution of the main taxa abundances corresponding to the different size fraction abundances counted by the ZOOSCAN (Fig. 2) are presented in Fig. 6 for the two visits of station A3, the Kerguelen central plateau bloom reference station, and for stations E3 and E5, in the stationary meander of the Polar front. The zooplankton community structure in A3-1 was numerically dominated by the medium size fraction (nearly comparable to the fraction 500–1000 µm to total abundance in Fig. 2) comprising more than 50 % of copepods, characterized by the abundant cyclopoïd *Oithona similis*, and completed along with unspecified calanoid copepodites, and the harpacticoid *Microsetella rosea*. The rest of this fraction included metanauplii of euphausiids, appendicularians, ostracods and small chaetognaths. The fraction "large size" mesozooplankton, similar to the 1000–2000 µm fraction counted with the ZOOSCAN and representing 10.7 % of the total abundance, was composed of 98 % copepods with some major taxa (*Ctenocalanus citer*, *Metridia lucens*, *Scolecithricella minor*, *Calanus simillimus*, *Scaphocalanus* spp., *Clausocalanus laticeps*), and early copepodites of *Paraeuchaeta* and of *Calanidae*. The highest size fraction was dominated for more than 75 % by *Rhincalanus gigas* and amphipods *Hyperia* spp. and *Themisto gaudicaudii*. It corresponds to the fraction > 2000 µm from the ZOOSCAN which contributes to two thirds of the mesozooplancton biomass at station A3-1 (see Fig. 2). The lowest size fraction was mainly composed by euphausiid eggs and nauplii, copepod nauplii, small forms of the pteropod *Limacina retroversa* and in small densities foraminifera and radiolarians. As a whole the mesozooplancton community in A3-1 was mainly composed by herbivorous species in all fractions, such as the copepods *R. gigas*, *C. citer*, *O. similis*, *M. rosea*, but also pteropod *L. retroversa*, appendicularians and different nauplii stages of copepods and euphausiids. In lowest densities, omnivores and detritivores (such as the copepods *M. lucens*, *S. minor*, *C. simillimus*) and carnivores (such as chaetognaths and amphipods, and the copepod *Paraeuchaeta*) were found.

During the second visit at the station A3 (A3-2), the relative total abundance was dominated by fractions with ECD < 1000 µm (up to 83 % of the total abundance, see in Fig. 3). The taxa distribution in A3-2 differed from the first visit (station A3-1) by an

BGD
12, 2381–2427, 2015

increase of copepod nauplii and euphausiid eggs in the "small" size fractions, and appendicularians and early copepodid stages of copepods for the second in the "medium" size fraction. The two largest fractions ("large" and "very large") were not very different in A3-1 and A3-2 in taxonomic composition and distribution (the only difference being the apparition of late larval stages of euphausiid in the "very large" fraction).

The major features in taxonomic changes between the station E3 (4 November) and E5 (18 November) (Fig. 6) were the increasing contribution of calanoid copepodids in the medium and large size fractions with the concomitant increase of these fractions to the total abundance (see also Fig. 2), and the increase of euphausiid larvae in the largest fraction. The smaller fraction presented a rather stable distribution of dominant taxa, with copepod nauplii and *Limacina* as dominant groups (Fig. 6). As a whole, if omnivores, carnivores and scavengers are present, the herbivorous component is largely dominant with all these larval forms. It is interesting to note that the dominant species for the different fractions in E5 were quite similar to those in A3-1, but with the noticeable difference that many larval stages occurred in all size fractions, inducing the highest observed abundance during the survey (see Fig. 2), although finally representing lower biomass (see Fig. 3).

To compare the taxonomic composition between all stations, a cluster dendrogram quantifying the compositional similarity of taxa distributions between the different stations was built from the Bray–Curtis coefficient (Fig. 7). This analysis showed a high degree of similarity across the whole region related to the initial phase of zooplankton development. The shelf stations presented the highest level of dissimilarity compared to the other stations.

The cluster dendrogram sliced at 80 % similarity allowed to distinguish two BC-groups: a first one grouping (BC-Group 1, with more than 80 % similarity) the oceanic stations within the PF meander and including eastern stations east of PF (FL and TW7), and a second group of dispersed stations (BC-Group 2, with less than 80 % similarity – differences in day-night samplings being not considered in this analysis), including the R2 station on the western side of the Kerguelen plateau characterized by higher abun-

BGD
12, 2381–2427, 2015

dance of large calanoid copepods such as *Rhincalanus gigas* and *Paraeuchaeta* spp., the TEW1 and TEW2 stations, near the Kerguelen coast and dominated by *Drepanopus pectinatus* and bivalvia meroplanktonic larvae, the TNS1and TNS2 stations in Subantarctic Surface Water waters dominated by medium size cyclopoid and calanoids and larval forms of euphausiids, the A3 and TNS10 stations in the southern part (see detail below), and the stations TEW3, TEW5, TEW8, which were characterized by relative differences in very few taxa compared to other stations of the TEW transect (high density of *Metridida lucens* in TEW3, relative lower density of *Ctenocalanus citer* in TEW5, and high density of *Triconia* sp. in TEW8).

3.3 Isotopic composition of size-fractionated zooplankton and within zooplankton taxa

A large range of δ^{13}C (> 8 ‰) and δ^{15}N (> 4 ‰) values were recorded among zooplankton size-fractions and stations (Table 2). A slight general increase of δ^{13}C with increasing size-fraction was observed, while the difference was not significant due to large differences among sites ($F = 1.818$, $p = 0.132$) (Fig. 8a). A significant increase in δ^{15}N with increasing size was observed ($F = 11.67$, $p < 0.001$), particularly between the two smallest fractions (80–200 µm and 200–500 µm) and the 3 largest ones (Fig. 8b). However, no significant difference in mean δ^{15}N occurred between the 500–1000 µm and > 2000 µm fractions, while the 1000–2000 µm fraction exhibited a slightly lower δ^{15}N than the two others. Within each size-fraction, no difference was observed between mean day and night δ^{13}C and δ^{15}N values ($p > 0.05$ for both), in spite of differences at site level (Table 2). Thus, for both δ^{13}C and δ^{15}N values, the main difference occurred between the two smallest size classes (< 500 µm) and the three largest ones (> 500 µm).

At the station level, mean δ^{13}C and δ^{15}N values differed, resulting in three isotopic groups of stations (IS-Groups) individualised by hierarchical cluster analysis (Fig. 9). Station R2 (IS-Group 1) presented the lowest mean δ^{13}C (–25.26 ‰) and the highest mean δ^{15}N (4.49 ‰), while stations FL, TEW-8 and E4-E (IS-Group 3) were charac-

BGD
12, 2381–2427, 2015

terized by the highest δ^{13}C (> −21.2 ‰) and rather high δ^{15}N values (> 4 ‰). All the other stations (IS-Group 2) exhibited mean δ^{13}C values (from −23.26 ‰ to −21.76 ‰) and a large range of δ^{15}N values (from 3.63 ‰ to 4.25 ‰). Trull et al. (2014) considered 5 groups of stations (T-Groups) based on chemometric measurements. Station R2 (IS-Group 1) belonged to T-Group1, while stations included in IS-Group 3 belonged to T-Group 5 (except station E4-E). Stations gathered in IS-Group 2 (Fig. 9) belonged to T-Group 1, T-Group 2 and T-Group 3.

Difference in mean δ^{15}N among small (< 500 µm) and large (> 500 µm) zooplankton size-fractions were low in T-Group 1 (0.3 ‰), increased in T-Group 5 (0.6 ‰) and were the highest in T-Group 2 and T-Group 3 (0.9 ‰) which gathered most stations located in the eddy (Fig. 10). This trend suggested higher food overlap among size-fraction in zooplankton associated with phytoplankton T-Group 1 and T-Group 5, and more partitioned food resources in phytoplankton T-Group 2 and T-Group 3, as indicated by a more even increase in δ^{15}N with zooplankton size in these stations (Fig. 10).

The smaller size-fraction (80–200 µm) was differently composed according to stations, being dominated either by diatoms (A3-2, E-4W), foraminifera (A3-1), small copepods (R2), or a mixture of these groups (most stations). Diatoms, foraminifera, pteropods thecosomes, eggs, detritus and copepods contributed to the 200–500 µm fraction. The following size-fractions (500–1000 µm, 1000–2000 µm and > 2000 µm) were all dominated by copepods (60–95 %), but amphipods, euphausiids, appendicularians and chaetognaths increased in abundance from the 500–1000 µm to the 1000–2000 µm fractions. The largest size-fraction (> 2000 µm) was dominated by *Rhincalanus gigas* and euphausiid larvae or juveniles. Large chaetognaths completed this large fraction.

Thus differences in specific composition of size-fractions, particularly in the smallest and the largest ones, could result in isotopic differences among stations within a size fraction. For example, when diatoms dominated the 80–200 µm fraction, δ^{15}N values were lower than when composed of foraminifera or small copepods (2–3 ‰ and 4–4.5 ‰, respectively).

BGD
12, 2381–2427, 2015

Groups of organisms individualized in the > 2000 µm fraction presented highly different isotopic signatures according to their main feeding behaviours (Table 3). Filtering salps presented the lowest δ^{15}N (< 4 ‰), the mostly herbivorous copepods, amphipods, euphausiids, and pteropods intermediate values (4 to 4.6 ‰), while predatory chaetognaths, fish larvae and polychaetes exhibited higher δ^{15}N values (> 5 ‰). Thus, δ^{15}N differences of the > 2000 µm fraction among stations resulted mainly from the relative contributions of these groups to bulk samples (ex: higher proportion of salps and euphausiids at A3-2, and large chaetognaths at E5). Accordingly, differences in δ^{13}C values could be linked to difference in both size and composition of the ingested food. The lower δ^{13}C recorded in gymnosomes and copepods suggested the consumption of small phytoplankton particles, while the higher δ^{13}C of euphausiids suggested a consumption of larger-sized phytoplankton. Higher δ^{13}C in euphausiids compared to copepods was also observed in Arctic seas (Schell et al., 1998).

4 Discussion

4.1 Zooplankton development during the early spring bloom in 2011 and comparison with other seasons

In high latitudes, zooplankton firstly increase in abundance more than biomass in response to initial phytoplankton spring bloom due to stimulated reproduction of overwintering adults of dominant copepods. This induces a lag-time in the grazing response of herbivorous zooplankton at the beginning of blooms, which further promotes the rapid phytoplankton accumulation. Higher phytoplankton concentrations then stimulate grazing by overwintering stages and new cohorts which results in build-up of zooplankton biomass. With the succession of new cohorts in the full bloom conditions (above 0.8 mg Chl a m^{-3}), continuous egg production and individual growth induce proportional increase of abundance and biomass.

BGD
12, 2381–2427, 2015

Such a response of zooplankton to an early phase of the bloom was observed in the bloom of the northeastern Kerguelen bloom during the pseudo-Lagrangian survey within the sampled stationary meander of the Polar Front (stations E1 to E5, except E4-W, Figs. 2–4). During the pseudo-Lagrangian survey within the meander, the measured integrated average Chl *a* concentrations were rather low (0.49 to 0.77 µg Chl *a* m^{-3}) and even lower in the previous weeks when these waters were sampled during the perpendicular large transects (Lasbleisz et al., 2014). The POC was constant in the surface layer until E3, with an average of 83 mg C m^{-3}, and then slightly higher in E4 and E5 (with an average up to 109 mg C m^{-3}) (Lasbleisz et al., 2014). Zooplankton densities increased from 60×10^3 ind m^{-2} (E1-d) to 200 10^3 ind m^{-2} (E5-d) whereas biomasses gradually decreased (excepted E4-E-n) from 2.3 g C m^{-2} (E1-d) to 1.7 g C m^{-2} (E5-n). Two processes may favor the shift towards smaller size classes. Firstly, the contribution of the larger size classes to biomass decreased with time (Fig. 3) due to the reduction of initial standing stock of overwintering zooplankton by mortality and by investment in egg production. The dominant overwintering copepods (*Ctenocalanus citer*, *Rhincalanus gigas*) are known to be strong seasonal migrants able to spawn in early spring even at low chlorophyll concentrations (Schnack-Schiel, 2001; Atkinson, 1998), i.e. before the full bloom conditions. Moreover, smaller copepods species and copepodids of large copepods may better exploit these low food concentrations (Atkinson et al., 1996) allowing individuals to develop and grow whereas large copepods are food limited.

The response to chlorophyll increase on waters above the plateau (station A3 on Fig. 4c) was more proportional in abundance and biomass (3-fold higher in A3-2 than in A3-1). Lasbleisz et al. (2014) mentions that the Chl *a* increase at station A3-2 was accompanied by an increase of the Phaeo: Chl *a* ratio reflecting a potential higher grazing activity. The mesozooplankton in A3-2 presented a grazer community structure able to feed on a large spectrum of cells from small diatoms to phytodetritus aggregates as observed at this station (Lasbleisz et al., 2014; Laurenceau et al., 2014), as well as small nano/microzooplankton (Christaki et al., 2014) and carnivorous zooplankton. Compared to A3-1, the medium size and small size mesozooplankton fractions had

BGD
12, 2381–2427, 2015

a much larger contribution of microphagous organisms (appendicularians, copepod nauplii,...) which could quickly remove the smaller planktonic forms (below 20 µm). The larger zooplankton size fractions were a mixture of efficient grazers on large diatoms (> 20 µm), omnivores and detritivores able to feed on aggregates, and carnivores consuming micro and mesozooplanckton. Later in the season during KEOPS1 (January-February) a similar mature zooplankton community structure was found and stayed rather stable during the second half of the bloom (Carlotti et al., 2008), but with biomasses more than twice as the biomasses observed at the end of November during KEOPS2.

The mesozooplankton biomass stocks observed at the beginning of the KEOPS2 cruise were around 2 g C m^{-2} both above the plateau (A3) and in oceanic waters (TNS transect). Oceanic biomass was almost unchanged during the cruise, excepted the biomass observed in the eastern bloom (station FL) in the Polar Front Zone (above 4 mg C m^{-2}), and station A3 presented also with biomass around 4 mg C m^{-2} at the end of the cruise. These different results during KEOPS2 suggest that the zooplankton community is able to respond to the growing phytoplankton blooms earlier on the plateau than in the oceanic waters, where complex mesoscale circulation stimulates initial more or less ephemeral blooms before a broader bloom extension. Due to a constrained sampling for these oceanic stations, it was not possible to identify if the observed zooplankton biomass variability between oceanic stations during the two transects was linked to enhanced local production (except for stations near the permanent polar front sustaining high level of production).

The pseudo-Lagrangian survey within the meander suggests that the heterogeneous primary production linked to oceanic mesoscale activity in the early spring bloom phase may stimulate the production of new zooplankton cohorts but cause reduced individual growth, slowing down the built-up of new zooplankton biomass. Moreover, potential predation on mesozooplankton by euphausiid populations could be expected from increasing contribution of larval stages in our bongo net samples (see Fig. 6) and observed long faecal pellets in gel traps (Laurenceau et al., 2014).

BGD
12, 2381–2427, 2015

Inversely, stations FL (6 November) and A2 (16 November) presented the highest biomasses (maintained below 5 g C m^{-2}) observed in November (Figs. 4 and 5) and a similar ratio of abundance on biomass, around 20×10^3 ind g C^{-1} (Fig. 4) and a lower contribution of smaller size-fractions (ESD < 1000 µm) to total biomass comparatively to station E5. These characteristics could be the results of a phytoplankton-sustained zooplankton development over the previous weeks.

4.2 Comparison to previous results

If we group our observations of KEOPS1 and KEOPS2, the zooplankton biomass in A3 doubled from mid-October to mid-November 2011, and further increased 2 to 3 fold higher between the values of mid-November 2011 and the summer values at the end of January 2011 (see Carlotti et al., 2008, their Fig. 3b). For the oceanic stations, the ratio of zooplankton biomass increase is in average of the same order although difficult to estimate due the strong variability of observed biomasses between stations for both surveys (see Fig. 2 in Carlotti et al., 1998). The comparison in terms of abundances is biased by the different counting devices, the Lab OPC used for the treatment of KEOPS1 samples having a lower size limit of detection (280 µm) than the ZOOSCAN used for KEOPS2 samples per (300 µm). The ratio between the values observed at the end of KEOPS1 and the beginning of KEOPS2 is around 5 for the A3 station and 2 to 3 for the oceanic stations, and might be explained by a longer sustained reproduction period over summer above the plateau than in oceanic conditions.

During the SKALP cruises, all around the Kerguelen Island (46–52° S, 64–73° E), Semelkina (1993, her Table 1) observed an increase from 62×10^3 ind m^{-2} in July-August 1987 (average values between 0 and 200 m depth for the whole sampled area, nearly the double from 0–1000 m) to 570×10^3 ind m^{-2} in February 1988 (values between 0 and 200 m, 100×10^3 ind m^{-2} additional in the layer 200–400 m). In term of biomass, assuming a carbon content to be 50 % of body dry weight, the biomass increase in the 200 upper meters was from 2.2 to 19 g C m^{-2}. The sampled areas during the SKALP cruises covered a much larger area than the one studied during KEOPS2,

BGD
12, 2381–2427, 2015

but theses average values corresponded to the one observed eastern side of the Kerguelen (see Semelkina, 1993, her Fig. 2). Concerning the taxonomic composition of the mesozooplankton, she mentioned no seasonal variations but differences in population development and distribution.

Razouls et al. (1998) presented the seasonal changes in copepods distributions at the KERFIX station, a fixed time-series station, situated 60 miles southwest of the Kerguelen Islands (50°40′ S, 68°25′ E), in 1700 m of water, characteristic of the Permanently Open Ocean Zone (POOZ). The copepod abundance sampled from vertical hauls (300 m – surface) started from less than 30×10^3 ind m^{-2} in winter and 45×10^3 ind m^{-2} in October up to 222×10^3 ind m^{-2} in January. The nearest station during KEOPS1 and 2 was the station R2 which presented biomasses (respectively abundance densities) of 10.7 g C m^{-2} (272×10^3 ind m^{-2}) in February 2005 and 4.5 g C m^{-2} (80×10^3 ind m^{-2}) in November 2011. Abundances during KEOPS1 and 2 were largely dominated (> 80 %) by copepods (Carlotti et al., 2008, their Fig. 7; distribution not shown for KEOPS2).

During a coastal annual survey in the Morbihan Bay at Kerguelen Islands, Razouls et al. (1996) found a ratio of 10 between winter and spring-summer mesozooplankton densities (from 2 to 20×10^3 ind m^{-3}) and a ratio of 20 for the corresponding biomass (from 20 to 400 mg DW m^{-3}).

In addition to the recent synthesis of the CPR data in the region (Hosie et al., 2003; Hunt and Hosie, 2006b) which show the important development of mesozooplankton abundance in October-November, the overall results of KEOPS 1 and 2 in term of seasonal changes in abundance and biomass values are very consistent with the information provided by Semelkina (1993) and Razouls et al. (1998).

4.3 Effects of primary production on trophic pathways through mesozooplankton

The KEOPS2 cruise illustrates the complexity of the phytoplankton bloom in spring in the oceanic waters of the Kerguelen Island linked to the intense mesoscale activity

BGD
12, 2381–2427, 2015

both in species diversity and spatial production. Comparatively the mesozooplankton presents an initial standing biomass stocks between 1 and 2 g C m^{-2} everywhere in the region, ready to exploit any new phytoplankton production. When this occurs, the initial response is to produce new cohorts which grow further as the bloom builds up, delaying the major grazing impact when these cohorts reach the later stages. Sustained full blooms in plateau stations or permanent fronts favor the highest and longest secondary production. The spring period usually show the largest increase in grazing pressure on phytoplankton (Razouls et al., 1998).

The comparison of the sinking particle composition at early and advanced stages of the bloom at station A3 (Laurenceau et al., 2014 for KEOPS2; Ebersbach et al., 2008 for KEOPS1) show that early bloom stage is characterized with particles dominated by phyto-aggregates due to relatively weak grazing pressure on phytoplankton stocks, whereas faecal aggregates characterized the vertical matter flux as soon as the zooplankton grazing affects substantially the phytoplankton stock.

The qualitative composition of the bloom had a direct impact in term of species dominance (mostly herbivorous species) and biochemical composition of the zooplankton organisms. The spatial differences observed in isotopic signatures of phytoplankton were tracked up to the higher zooplankton levels and showed the impact of the food source.

Differences in the isotopic ratios of zooplankton were observed among stations during KEOPS2 cruise, with three distinct isotopic groups. IS-Group 1 (R2) exhibited a 2.2 ‰ lower δ^{13}C than IS-Group 2, while δ^{13}C of IS-Group 3 was elevated by ~ 1.5 ‰ compared to IS-Group 2. A similar increase in carbon isotopic signature was observed by Trull et al. (2014) for phytoplankton, with the lowest δ^{13}C in the HNLC reference station (R2) and the highest ones in T-Group 5, corresponding respectively to zooplankton IS-Group 1 and IS-Group 3. Similarly, higher δ^{15}N were observed in corresponding phytoplankton (R2 and T-Group 5) and zooplankton (R2 and IS-Group 3) groups.

The mean increase in δ^{15}N in small zooplankton size classes (from 80–200 µm to 500–1000 µm) was higher than among larger size-fractions (from 500–1000 µm to

BGD
12, 2381–2427, 2015

> 2000 µm) (1 ‰ and 0.28 ‰ respectively). This lower increase in mean δ^{15}N from 500–1000 µm to > 2000 µm suggested a high food overlap among the three largest size-fractions, with a dominance of herbivorous organisms. Within the largest size fraction (> 2000 µm), an increase in trophic level (δ^{15}N) was observed from filtering (salps) and mostly herbivorous organisms (copepods, pteropods,. . .) to predatory carnivores (chaetognaths), as observed in other regions (Tarling et al., 2012; Banaru et al., 2014). While different feeding behaviours can be observed among euphausiids (Mauchline, 1980), most euphausiids collected during KEOPS2 cruise were mainly herbivores or omnivores with a δ^{15}N varying between 3.5 ‰ and 5.0 ‰ for individuals > 2000 µm, a range value already observed in Southern Ocean (Gurney et al., 2001; Schmidt et al., 2003). High feeding overlap across size-fractionated zooplankton is reported in most studies (Fry and Quiñones, 1994; Bode et al., 2007) and may increase during food shortage (Tarling et al., 2012; Banaru et al., 2014). During KEOPS2, the highest food overlap among zooplankton size-fractions seemed to be associated with phytoplankton T-Group 1 and T-Group 5 in which small-sized cells dominated, while more partitioned food resources among size-fractions seemed to occur in zooplankton associated with phytoplankton T-Group 2 and T-Group 3, where large phytoplankton cells dominated (Trull et al., 2014).The direct comparison between stable isotope values of size-fractionated zooplankton and their abundance or biomass in water masses is difficult. Zooplankton isotopic values are firstly related to those of the phytoplankton they feed on, themselves linked to water characteristics and nutrient cycling (Trull et al., 2014). However, the variations of isotopic signatures with time during KEOPS2 at stations A3 and E suggested an increase in herbivory in zooplankton after the development of the bloom and the increase in zooplankton abundance (particularly those of < 1000 µm fractions). Mean δ^{15}N decreased from A3-1 to A3-2, and in the meander from E2 to E5 (Fig. 9). In the meantime, an increase in the trophic enrichment index $\Delta\delta^{15}$N (i.e. the range of δ^{15}N values among size fractions at a station) was observed. $\Delta\delta^{15}$N increase from 1.68 ‰ at A3-1 to 3.74 ‰ at A3-2, and from 1.82 ‰ at E2 to 3.74 ‰ at E5. The decrease in δ^{15}N indicated a lower mean trophic level of the zoo-

BGD
12, 2381–2427, 2015

plankton community, while the increase in $\Delta\delta^{15}$N indicated a direct and better transfer of the production up to the food web. The two parameters combined strongly suggested a general increase in herbivory in zooplankton during the bloom in accordance with the increase in the abundance of small-sized zooplankton, and corroborated the finding of Lableisz et al. (2014) based on the Phaeo : Chl *a* ratio. Similar variations in isotopic signatures of zooplankton were observed in the Mediterranean after the phytoplankton spring bloom (Banaru et al., 2014). In contrast, the higher mean δ^{15}N and the lower $\Delta\delta^{15}$N observed at the beginning of the bloom during KEOPS2 (A3-1, E2) suggested that zooplankton organisms relied more on omnivory and the microbial loop during the winter food shortage.

5 Conclusions

The complexity of the oceanic processes inducing the large scale phytoplankton bloom in the eastern area of Kerguelen Island occurs over scales ranging from the very large (1000 of kilometers) down to the submesoscales (10 of kilometers) marked by intense oceanic–plateau interactions linked to the meandering circulation of the Polar Front (PF) and by a myriad of secondary circulations linked to circulations resulting in a patchy distribution of the new production with different intensity and duration. The KEOPS2 survey addressed the challenge to examine the large scale phytoplankton bloom that forms over and downstream of the Kerguelen plateau at the most productive season but also to observe at a finer resolution to understand the spatial and temporal variability of biogeochemical and biological processes on the overall regional ecosystem dynamics and carbon export.

Our results on the mesozooplankton dynamics during KEOPS2 suggest that the zooplankton community maintains relatively high winter stocks both on the plateau and in the oceanic waters, mostly distributed in mesopelagic waters, ready to exploit the early phytoplankton blooms. The timing and intensity of the bloom on the plateau allow an earlier and longer period favorable for zooplankton development and growth compared

BGD
12, 2381–2427, 2015

to the surrounding oceanic waters. A longer lag-time (several weeks) between an initial reproduction phase of the zooplankton organisms and its biomass increase, and thus its grazing impact, was clearly observed in oceanic waters.

Acknowledgements. We thank the project coordinator, S. Blain, and the chief scientist on board, B. Quéguiner, for inviting us to take part in the KEOPS2 project and for supplying data. We thank the captain Bernard Lassiette and crew of the R/V *Marion Dufresne* for their support aboard. We also thank P. Richard LIENSs Laboratory at the Université de La Rochelle for valuable advice on stable isotope analysis, and Tom Trulls and Marc Pagano for valuable comments on the manuscript.

This work was supported by the French Research program of INSU-CNRS LEFE–CYBER ("Les enveloppes fluides et l'environnement – Cycles biogéochimiques, environnement et ressources"), the French ANR (Agence Nationale de la Recherche, ANR-10-BLAN-0614 of SIMI-6 program, and ANR-09-CEXC-006-01 to M. Zhou and F. Carlotti), the French CNES (Centre National d'Etudes Spatiales) and the French Polar Institute IPEV (Institut Polaire Paul-Emile Victor).

References

Atkinson, A.: Life cycle strategies of epipelagic copepods in the Southern Ocean, J. Marine Syst., 15, 1–4, 289–311, 1998.

Atkinson, A., Shreeve, R. S., Pakhomov, E. A., Priddle, J., Blight, S. P., and Ward, P.: Zooplankton response to a phytoplankton bloom near South Georgia, Antarctica, Mar. Ecol.-Prog. Ser., 144, 195–210, 1996.

Banaru, D., Carlotti, F., Barani, A., Gregory, G., Neffati, N., and Harmelin-Vivien, M.: Seasonal variation of stable isotope ratios of size-fractionated zooplankton in the Bay of Marseille (NW Mediterranean Sea), J. Plankton Res., 36, 145–156, 2014.

Blain, S., Quéguiner, B., Armand, L., Belviso, S., Bombled, B., Bopp, L., Bowie, A., Brunet, C., Brussaard, C., Carlotti, F., Christaki, U., Corbiere, A., Durand, I., Ebersbach, F., Fuda, J. L., Garcia, N., Gerringa, L., Griffiths, B., Guigue, C., Guillerm, C., Jacquet, S., Jeandel, C., Laan, P., Lefèvre, D., Lo Monaco, C., Malits, A., Mosseri, J., Obernosterer, I., Park, Y. H., Picheral, M., Pondaven, P., Remenyi, T., Sandroni, V., Sarthou, G., Savoye, N.,

BGD
12, 2381–2427, 2015

Scouarnec, L., Souhaut, M., Thuiller, D., Timmermans, K., Trull, T., Uitz, J., van Beek, P., Veldhuis, M., Vincent, D., Viollier, E., Vong, L., and Wagener, T.: Effect of natural iron fertilization on carbon sequestration in the southern ocean, Nature, 446, 1070–1074, 2007.

Blain, S., Quéguiner, B., and Trull, T.: The natural iron fertilization experiment KEOPS (Kerguelen Ocean and Plateau Compared Study): an overview, Deep-Sea Res. Pt. II, 55, 559–565, 2008.

Blain, S., Renaut, S., Xing, X., Claustre, H., and Guinet, C.: Instrumented elephant seals reveal the seasonality in chloropyll and light-mixing regime in the iron fertilized Southern Ocean, Geophys. Res. Lett., 40, 1–5, 2013.

Blain, S., Capparos, J., Guéneuguès, A., Obernosterer, I., and Oriol, L.: Distributions and stoichiometry of dissolved nitrogen and phosphorus in the iron fertilized region near Kerguelen (Southern Ocean), Biogeosciences Discuss., 11, 9949–9977, doi:10.5194/bgd-11-9949-2014, 2014.

Bode, A., Alvarez-Ossorio, M. T., Cunha, M. E., Garrido, S., Peleteiro, J. B., Porteiro, C., Valdés, L., and Varela, M.: Stable nitrogen isotope studies of the pelagic food web on the Atlantic shelf of the Iberian Peninsula, Prog. Oceanogr., 74, 115–131, 2007.

Bodin, N., Le Loc'h, F., and Hily, C.: Effect of lipid removal on carbon and nitrogen stable isotope ratios in crustacean tissues, J. Exp. Mar. Biol. Ecol., 341, 168–175, 2007.

Bray, J. R. and Curtis, J. T.: An ordination of the upland forest communities of southern Wisconsin, Ecol. Monogr., 27, 273–279, 1957.

Carlotti, F., Botha, D., Nowaczyck, A., and Lefèvre, D.: Structure, biomass, feeding and respiration of the mesozooplankton community during KEOPS, Deep-Sea Res. Pt. II, 55, 720–733, 2008.

Christaki, U., Lefèvre, D., Georges, C., Colombet, J., Catala, P., Courties, C., Sime-Ngando, T., Blain, S., and Obernosterer, I.: Microbial food web dynamics during spring phytoplankton blooms in the naturally iron-fertilized Kerguelen area (Southern Ocean), Biogeosciences, 11, 6739–6753, doi:10.5194/bg-11-6739-2014, 2014.

Clarke, K. R. and Warwick, R. M.: Change in Marine Communities: an Approach to Statistical Analysis and Interpretation, 2nd edn., Primer-E Ltd, Plymouth, UK, 2001.

Closset, I., Lasbleiz, M., Leblanc, K., Quéguiner, B., Cavagna, A.-J., Elskens, M., Navez, J., and Cardinal, D.: Seasonal evolution of net and regenerated silica production around a natural Fe-fertilized area in the Southern Ocean estimated with Si isotopic approaches, Biogeosciences, 11, 5827–5846, doi:10.5194/bg-11-5827-2014, 2014.

BGD
12, 2381–2427, 2015

De Niro, M. J. and Epstein, S.: Influence of diet on the distribution of carbon isotopes in animals, Geochim. Cosmochim. Ac., 42, 495–506, 1978.
d'Ovidio, F., Della Penna, A., Trull, T. W., Nencioli, F., Pujol, I., Rio, M. H., Park, Y.-H., Cotté, C., Zhou, M., and Blain, S.: The biogeochemical structuring role of horizontal stirring: Lagrangian perspectives on iron delivery downstream of the Kerguelen plateau, Biogeosciences Discuss., 12, 779–814, doi:10.5194/bgd-12-779-2015, 2015.
Ebersbach, F. and Trull, T. W.: Sinking particle properties from polyacrylamide gels during KEOPS: controls on carbon export in an area of persistent natural iron inputs in the Southern Ocean, Limnol. Oceanogr., 53, 212–224, doi:10.4319/lo.2008.53.1.0212, 2008.
Farías, L., Florez-Leiva, L., Besoain, V., and Fernández, C.: Dissolved greenhouse gases (nitrous oxide and methane) associated with the natural iron-fertilized Kerguelen region (KEOPS 2 cruise) in the Southern Ocean, Biogeosciences Discuss., 11, 12531–12569, doi:10.5194/bgd-11-12531-2014, 2014.
Fry, F. and Quiñones, R. B.: Biomass spectra and stable isotope indicators of trophic level in zooplankton of the northwest Atlantic, Mar. Ecol.-Prog. Ser., 112, 201–204, 1994.
Gorsky, G., Ohman, M. D., Picheral, M., Gasparini, S., Stemmann, L., Romagnan, J. B., Cawood, A., Pesant, S., Garcia-Comas, C., and Prejger, F.: Digital zooplankton image analysis using the ZooScan integrated system, J. Plankton Res., 32, 285–303, 2010.
Grosjean, P., Picheral, M., Warembourg, C., and Gorsky, G.: Enumeration, measurement, and identification of net zooplankton samples using the ZOOSCAN digital imaging system, ICES J. Mar. Sci., 61, 518–525, 2004.
Gurney, L. J., Froneman, P. W., Pakhomov, E. A., and McQuaid, C. D.: Trophic positions of three euphausiid species from the Prince Edward Islands (Southern Ocean): implications for the pelagic food web structure, Mar. Ecol.-Prog. Ser., 217, 167–174, 2001.
Hindell, M. A., Bost, C. A., Charrassin, J. B., Gales, N., Lea, M. A., Goldsworthy, S., Page, B., Robertson, G., Wienecke, W., O'Toole, M., and Guinet, C.: Foraging habitats of top predators, and areas of ecological significance, on the Kerguelen Plateau, in: The Kerguelen Plateau: Marine Ecosystem and Fisheries, edited by: Duhamel, G. and Welsford, D., Société d'Ichtyologie, Paris, 203–215, 2011.
Hosie, G. W., Fukuchi, M., and Kawaguchi, S.: Development of the Southern Ocean Continuous Plankton Recorder Survey, Prog. Oceanogr., 58, 263–283, 2003.

BGD
12, 2381–2427, 2015

Hunt, B. P. V. and Hosie, G. W.: Seasonal zooplankton community succession in the Southern Ocean south of Australia, Part I: The seasonal ice zone, Deep-Sea Res. Pt. I, 53, 1182–1202, 2006a.
Hunt, B. P. V. and Hosie, G. W.: Seasonal zooplankton community succession in the Southern Ocean south of Australia, Part II: The sub-antarctic to polar frontal zones, Deep-Sea Res. Pt. I, 53, 1203–1223, 2006b.
Jacquet, S. H. M., Dehairs, F., Cavagna, A. J., Planchon, F., Monin, L., André, L., Closset, I., and Cardinal, D.: Early season mesopelagic carbon remineralization and transfer efficiency in the naturally iron-fertilized Kerguelen area, Biogeosciences Discuss., 11, 9035–9069, doi:10.5194/bgd-11-9035-2014, 2014.
Jouandet, M.-P., Jackson, G. A., Carlotti, F., Picheral, M., Stemmann, L., and Blain, S.: Rapid formation of large aggregates during the spring bloom of Kerguelen Island: observations and model comparisons, Biogeosciences, 11, 4393–4406, doi:10.5194/bg-11-4393-2014, 2014.
Lasbleiz, M., Leblanc, K., Blain, S., Ras, J., Cornet-Barthaux, V., Hélias Nunige, S., and Quéguiner, B.: Pigments, elemental composition (C, N, P, and Si), and stoichiometry of particulate matter in the naturally iron fertilized region of Kerguelen in the Southern Ocean, Biogeosciences, 11, 5931–5955, doi:10.5194/bg-11-5931-2014, 2014.
Laurenceau, E. C., Trull, T. W., Davies, D. M., Bray, S. G., Doran, J., Planchon, F., Carlotti, F., Jouandet, M.-P., Cavagna, A.-J., Waite, A. M., and Blain, S.: The relative importance of phytoplankton aggregates and zooplankton fecal pellets to carbon export: i nsights from free-drifting sediment trap deployments in naturally iron-fertilised waters near the Kerguelen plateau, Biogeosciences Discuss., 11, 13623–13673, doi:10.5194/bgd-11-13623-2014, 2014.
Lee, R. F., Hagen, W., and Kattner, G.: Lipid storage in marine zooplankton, Mar. Ecol.-Prog. Ser., 307, 273–306, 2006.
Mauchline, J.: The biology of euphausiids, Adv. Mar. Biol., 18, 370–637, 1980.
Motoda, S.: Device of simple plankton apparatus, Mem. Fac. Fish. Hokkaido Univ., 7, 73–94, 1959.
Nowaczyk, A., Carlotti, F., Thibault-Botha, D., and Pagano, M.: Distribution of epipelagic metazooplankton across the Mediterranean Sea during the summer BOUM cruise, Biogeosciences, 8, 2159–2177, doi:10.5194/bg-8-2159-2011, 2011.
Park, Y.-H., Durand, I., Kestenare, E., Rougier, G., Zhou, M., d'Ovidio, F., Cotté, C., and Lee, J.-H.: Polar front around the Kerguelen Islands: an up-to-date determination and asso-

BGD
12, 2381–2427, 2015

ciated circulation of surface/subsurface waters, J. Geophys. Res.-Oceans, 119, 6575–6592, doi:10.1002/2014JC010061, 2014.
Post, D. M., Layman, C. A., Arrington, D. A., Takimoto, G., Quattrochi, J., and Montaña, C. G.: Getting to the fat of the matter: models, methods and assumptions for dealing with lipids in stable isotope analyses, Oecologia, 152, 179–189, 2007.
Quéguiner, B.: Iron fertilization and the structure of planktonic communities in high nutrient regions of the Southern Ocean, Deep-Sea Res. Pt. II, 90, 43–54, 2013.
Razouls, C., de Bovée, F., Kouwenberg, J., and Desreumaux, N.: Diversity and Geographic Distribution of Marine Planktonic Copepods, available at: http://copepodes.obs-banyuls.fr/en (last access: 25 January 2015), 2014.
Razouls, S., Koubbi, P., and Mayzaud, P.: Spatio-temporal distribution of mesozooplankton in a sub-Antarctic coastal basin of the Kerguelen Archipelago (southern Indian Ocean), Polar Biol., 16, 581–587, 1996.
Razouls, S., Du Réau, G., Guillot, P., Maison, J., and Jeandel, C.: Seasonal abundance of copepod assemblage and grazing pressure in the Kerguelen Island area (Southern Ocean), J. Plankton Res., 20, 1599–1614, 1998.
Riandey, V., Champalbert, G., Carlotti, F., Taupier-Letage, I., and Thibault-Botha, D.: Zooplankton distribution related to the hydrodynamic features in the Algerian Basin (western Mediterranean Sea) in summer 1997, Deep-Sea Res. Pt. I, 52, 2029–2048, 2005.
Rose, M.: Copépodes pélagiques, Faune de France, 26, Ed. Lechevalier, Paris, 374 pp., 1933.
Sackett, O., Armand, L., Beardall, J., Hill, R., Doblin, M., Connelly, C., Howes, J., Stuart, B., Ralph, P., and Heraud, P.: Taxon-specific responses of Southern Ocean diatoms to Fe enrichment revealed by synchrotron radiation FTIR microspectroscopy, Biogeosciences, 11, 5795–5808, doi:10.5194/bg-11-5795-2014, 2014.
Schell, D. M., Barnett, B. A., and Vinette, K. A.: Carbon and nitrogen isotope ratios in zooplankton of the Bering, Chukchi and Beaufort seas, Mar. Ecol.-Prog. Ser., 162, 11–23, 1998.
Schmidt, K., Atkinson, A., Stubing, D., McClelland, J. W., Montoya, J. P., and Voss, M.: Trophic relationships among Southern Ocean copepods and krill: some uses and limitations of a stable isotope approach, Limnol. Oceanogr., 48, 277–289, 2003.
Schnack-Schiel, S. B.: Aspects of the study of the life cycles of Antarctic copepods, Hydrobiology, 453–454, 9–24, 2001.
Schultes, S. and Lopes, R. B.: Laser optical plankton counter and ZooScan intercomparison in tropical and subtropical marine ecosystems, Limnol. Oceanogr.-Meth., 7, 771–784, 2009.

BGD
12, 2381–2427, 2015

Semelkina, A. N.: Development of the zooplankton in the Kerguelen Island region in the years 1987–1988, in: Campagnes SKALP 1987 et 1988 aux îles Kerguelen à bord des navires "SKIF" et "KALPER", edited by: Duhamel, G., Institut Français pour la recherche et la technologie polaires, Rapports des campagnes à la mer 93–01, Paris, 90–103, 1993.

Soreide, J. E., Tamelander, T., Hop, H., Hobson, K. A., and Johansen, I.: Sample preparation effects on stable C and N isotope values: a comparison of methods in Arctic marine food web studies, Mar. Ecol.-Prog. Ser., 328, 17–28, 2006.

Tarling, G. A., Stowasser, G., Ward, P., Poulton, A. J., Zhou, M., Venables, H. J., McGill, R. A. R., and Murphy, E. J.: Seasonal trophic structure of the Scotia Sea pelagic ecosystem considered through biomass spectra and stable isotope analysis, Deep-Sea Res. Pt. II, 59–60, 222–236, 2012.

Trégouboff, G. and Rose, M.: Manuel de planctonologie méditerranéenne, Centre National de la Recherche Scientifique, Paris, 587 pp., 1957.

Trull, T. W., Davies, D. M., Dehairs, F., Cavagna, A.-J., Lasbleiz, M., Laurenceau, E. C., d'Ovidio, F., Planchon, F., Leblanc, K., Quéguiner, B., and Blain, S.: Chemometric perspectives on plankton community responses to natural iron fertilization over and downstream of the Kerguelen Plateau in the Southern Ocean, Biogeosciences Discuss., 11, 13841–13903, doi:10.5194/bgd-11-13841-2014, 2014.

Wishner, K. F., Gelfman, C., Gowing, M. M., Outram, D. M., Rapien, M., and Williams, R. L.: Vertical zonation and distributions of calanoid copepods through the lower oxycline of the Arabian Sea oxygen minimum zone, Prog. Oceanogr., 78, 163–191, 2008.

Zhou, M., Zhu, Y., d'Ovidio, F., Park, Y.-H., Durand, I., Kestenare, E., Sanial, V., Van-Beek, P., Queguiner, B., Carlotti, F., and Blain, S.: Surface currents and upwelling in Kerguelen Plateau regions, Biogeosciences Discuss., 11, 6845–6876, doi:10.5194/bgd-11-6845-2014, 2014.

BGD
12, 2381–2427, 2015

Table 1. List of zooplanktonic taxa collected and identified during the 2011 KEOPS2 cruise. Index of abundances: 1: rare; 2: low abundances ($< 1\,\mathrm{ind\,m^{-3}}$) but observed in many stations; 3: medium abundances ($1\,\mathrm{ind\,m^{-3}} < \# < 5\,\mathrm{ind\,m^{-3}}$); 4: high abundances ($\# > 5\,\mathrm{ind\,m^{-3}}$); 5: locally abundant ($\# > 5\,\mathrm{ind\,m^{-3}}$).

	Adult forms	Copepodites stages	Nauplii stages
Copepods			
Oithona similis	3		
Oithona frigida	4	} 3	
Microsetella rosea	2		
Oncaea spp.	2	2	
Triconia sp.	3		
Clausocalanus laticeps	3	2	
Ctenocalanus citer	4	4	
Microcalanus pygmaeus	2		
Metridia lucens	4	4	
Calanus propinquus	2	2	
Calanus simillimus	3	3	
Calanoides acutus	2	2	
Scolecithricella minor	4	3	
Scaphocalanus spp.	2	3	
Drepanopus pectinatus	5	5	
Pleuromamma robusta	2	2	
Candacia maxima	1	1	
Heterorhabdus spp.	1	1	
Aetideus armatus	1	4	
Haloptilus oxycephalus	1	4	
Paraeuchaeta spp.	2	4	
Rhincalanus gigas	3	3	3
Subeucalanus longiceps	2	2	2
Euchirella rostramagna	1		
Gaetanus pungens	1		
Undeuchaeta incisa	1		
Undetermined Nauplii			3
Undetermined C1-C2 Calanidae		3	
Undetermined C3-C5 Calanidae		3	

BGD
12, 2381–2427, 2015

Table 1. Continued.

	Adult forms	Larval forms	Eggs
Euphausiids			
Undetermined species	2	4	4
Ostracods	4		
Isopods	1		
Mysid			1
Decapod			1
Amphipods			
Themisto gaudicaudii	3		
Hyperia spp.	3		
Primno macropa	1		
Vibilia sp.	1		
Scina sp.	1		
Molluscs			
Limacina retroversa	4		
Limacina helicina	1		
Spongiobranchaea sp.	1		
Clio sp.	1		
Polychaetes			
Pelagobia sp.	2		
Tomopteris spp.	1		
Travisiopsis sp.	1		
Undetermined		3	
Appendicularians			
Thaliacea	1		
Salpa thompsoni	1		
Pyrosomid	1		
Ctenophores			
Cnidarians			
Undetermined larvae	1	1	
Undetermined adult	1		
Bougainvillia sp.	1		
Dimophyes arctica	1		
Pyrostephos vanhoeffeni	1		
Rosacea plicata	1		
Muggiaea bargmannae	1		
Solmundella bitentaculata	1		
Pegantha sp.	1		
Chaetognaths	4		
Radiolarians	3		
Foraminifera	4		
Meroplankton			
Cirripedia		1	
Echinodermata		1	1
Fish		1	
Mysid		1	
Polychaeta		1	
Bivalvia		1	

BGD
12, 2381–2427, 2015

Table 2. Isotopic composition of size-fractionated zooplankton (mean and SD). Mean δ^{13}C: values of acidified samples, mean δ^{13}C-norm.: lipid-normalised values (except for the lowest size-fraction), mean δ^{15}N: values of untreated samples.

Station Date	Fraction µm	mean δ^{13}C ‰PDB	SD δ^{13}C ‰PDB	mean δ^{13}C-norm. ‰PDB	SD δ^{13}C-norm. ‰PDB	mean δ^{15}N ‰air	SD δ^{15}N ‰air	C/N mass
A3-1 day	80	−25.52	0.10	−25.52	0.06	4.01	0.05	5.31
20 Oct 2011	200	-26.48	0.05	−24.00	0.08	4.89	0.12	5.85
	500	−26.20	0.05	−23.10	0.07	4.87	0.02	6.48
	1000	−24.52	0.14	−22.67	0.12	3.21	0.07	5.22
	2000	−25.16	0.03	−22.97	0.03	3.58	0.05	5.57
TNS-7 day	80	−23.26	0.06	−23.26	0.07	3.45	0.09	4.55
22 Oct 2011	200	−25.18	0.03	−23.70	0.02	3.41	0.15	4.85
	500	−25.74	0.06	−23.29	2.00	4.29	0.04	5.82
	1000	−24.76	0.01	−23.03	0.00	4.21	0.06	5.10
	2000	−25.84	0.03	−23.21	0.06	4.60	0.22	6.01
R-2 day	80	−27.93	0.02	−27.93	0.03	4.36	0.08	4.87
26 Oct 2011	200	−27.69	0.07	−25.84	0.10	4.97	0.03	5.23
	500	−27.11	0.06	−24.93	0.15	4.79	0.19	5.55
	1000	−26.43	0.10	−24.52	0.11	3.24	0.06	5.28
	2000	−26.15	0.06	−24.59	0.03	5.09	0.10	4.93
E-1 night	80	−23.61	0.05	−23.61	0.06	3.62	0.23	4.70
30 Oct 2011	200	−25.37	0.04	−23.91	0.03	3.04	0.05	4.83
	500	−25.73	0.03	−23.26	0.03	3.67	0.03	5.85
	1000	−25.26	0.05	−22.80	0.05	3.58	0.01	5.84
	2000	−26.27	0.03	−22.75	0.08	4.69	0.32	6.91
E-2 day	80	−24.62	0.04	−24.62	0.12	3.93	0.19	4.89
1 Nov 2011	200	−25.86	0.02	−23.48	0.09	3.83	0.03	5.75
	500	−25.70	0.04	−22.77	0.08	4.38	0.08	6.32
	1000	−25.54	0.02	−22.45	0.01	3.65	0.11	6.47
	2000	−26.12	0.02	−22.74	0.14	5.48	0.15	6.77
TEW-4 day	80	−25.15	0.01	−25.15	0.05	4.06	0.11	4.67
1 Nov 2011	200	−25.98	0.01	−24.73	0.02	3.61	0.23	4.62
	500	−25.23	0.02	−23.39	0.02	3.24	0.06	5.21
	1000	−26.01	0.03	−21.98	0.04	3.50	0.07	7.42
	2000	−27.02	0.06	−21.52	0.04	5.23	0.03	8.90
TEW-8 day	80	−22.58	0.05	−22.58	0.04	3.88	0.03	5.24
2 Nov 2011	200	−23.29	0.03	−21.00	0.04	3.90	0.03	5.67
	500	−23.73	0.04	−21.62	0.07	4.28	0.08	5.48
	1000	−23.60	0.07	−21.73	0.08	4.30	0.04	5.24
	2000	−23.29	0.05	−21.61	0.05	3.78	0.02	5.05
E-3 night	80	−24.70	0.02	−24.70	0.03	3.02	0.13	4.84
3 Nov 2011	200	−25.79	0.02	−23.52	0.03	3.50	0.04	5.65
	500	−25.60	0.02	−23.24	0.03	4.14	0.07	5.74
	1000	−25.67	0.03	−22.63	0.11	3.67	0.02	6.42
	2000	−25.62	0.04	−23.20	0.03	4.58	0.35	5.79
E-3 day	80	−24.82	0.04	−24.82	0.07	2.98	0.10	4.71
4 Nov 2011	200	−25.99	0.02	−23.51	0.05	3.58	0.06	5.85
	500	−26.26	0.02	−22.79	0.05	3.90	0.04	6.86
	1000	−25.57	0.03	−22.41	0.03	3.68	0.06	6.54
	2000	−26.71	0.03	−22.19	0.06	5.23	0.48	7.92

BGD
12, 2381–2427, 2015

Table 2. Continued.

Station Date	Fraction µm	mean $\delta^{13}C$ ‰PDB	SD $\delta^{13}C$ ‰PDB	mean $\delta^{13}C$-norm. ‰PDB	SD $\delta^{13}C$-norm. ‰PDB	mean $\delta^{15}N$ ‰air	SD $\delta^{15}N$ ‰air	C/N mass
FL day	80	−23.69	0.03	−23.69	0.05	3.66	0.09	5.87
6 Nov 2011	200	−24.06	0.01	−21.42	0.06	4.20	0.10	6.02
	500	−24.59	0.03	−21.62	0.14	5.08	0.08	6.35
	1000	−24.31	0.03	−21.58	0.07	4.44	0.10	6.11
	2000	−24.64	0.01	−21.48	0.04	5.00	0.17	6.55
FL night	80	−21.77	0.02	−21.77	0.01	4.06	0.10	4.80
6 Nov 2011	200	−23.41	0.03	−20.96	0.03	3.54	0.03	5.83
	500	−24.67	0.08	−21.01	0.12	4.41	0.09	7.05
	1000	−23.75	0.05	−21.58	0.06	4.06	0.05	5.54
	2000	−22.38	0.01	−21.53	0.02	3.61	0.06	4.21
E-4W day	80	−23.26	0.08	−23.26	0.02	3.17	0.12	5.14
11 Nov 2011	200	−24.66	0.05	−22.93	0.05	3.43	0.11	5.10
	500	−25.05	0.02	−22.70	0.02	3.85	0.07	5.73
	1000	−24.21	0.02	−22.31	0.08	3.97	0.08	5.28
	2000	−25.01	0.02	−21.38	0.01	4.64	0.17	7.53
E-4W night	80	−23.24	0.03	−23.24	0.05	2.97	0.29	4.72
11 Nov 2011	200	−24.83	0.07	−23.10	0.13	3.33	0.06	5.09
	500	−25.30	0.06	−22.81	0.06	3.94	0.02	5.86
	1000	−24.83	0.07	−22.52	0.04	3.91	0.04	5.68
	2000	−24.92	0.06	−22.10	0.07	3.85	0.12	6.20
E-4E night	80	−23.47	0.04	−23.47	0.04	2.42	0.14	5.14
12 Nov 2011	200	−25.24	0.04	−22.59	0.10	3.77	0.06	6.03
	500	−26.07	0.04	−19.61	0.06	4.72	0.14	9.88
	1000	−26.02	0.07	−18.92	0.45	4.82	0.20	10.53
	2000	−27.12	0.11	−17.64	0.26	4.76	0.59	12.93
E-4E day	80	−23.65	0.02	−23.65	0.03	3.17	0.52	5.53
13 Nov 2011	200	−25.32	0.06	−21.90	0.11	4.02	0.15	6.81
	500	−25.97	0.02	−20.81	0.17	4.40	0.08	8.56
	1000	−25.38	0.08	−21.06	0.21	4.63	0.08	7.72
	2000	−25.76	0.11	−22.67	0.09	3.96	0.49	6.48
A3-2 day	80	−22.82	0.09	−22.82	0.22	1.71	0.17	4.49
16 Nov 2011	200	−23.58	0.02	−22.42	0.05	3.89	0.02	4.53
	500	−24.19	0.04	−22.38	0.15	5.45	0.16	5.19
	1000	−23.44	0.05	−21.91	0.04	4.66	0.07	4.89
	2000	−23.09	0.04	−21.42	0.07	3.71	0.20	5.04
A3-2 night	80	−22.42	0.02	−22.42	0.06	2.43	0.09	4.44
16 Nov 2011	200	−23.47	0.04	−22.31	0.09	3.98	0.16	4.53
	500	−23.98	0.05	−22.33	0.16	4.90	0.06	5.02
	1000	−24.99	0.04	−20.38	0.10	5.04	0.04	8.01
	2000	−23.22	0.05	−21.46	0.04	4.11	0.06	5.13
E-5 day	80	−25.88	0.06	−25.88	0.09	2.45	0.01	3.71
18 Nov 2011	200	−26.64	0.36	−23.91	0.30	3.10	0.22	6.11
	500	−26.01	0.03	−23.04	0.04	3.24	0.17	6.35
	1000	−25.89	0.05	−23.00	0.09	3.30	0.02	6.27
	2000	−27.74	0.01	−21.59	0.20	6.19	0.14	9.56
E-5 night	80	−26.18	0.03	−26.18	0.07	2.87	0.27	6.01
19 Nov 2011	200	−25.90	0.02	−22.64	0.05	3.45	0.09	6.64
	500	−26.07	0.01	−22.54	0.04	3.61	0.02	6.92
	1000	−25.90	0.04	−22.71	0.09	3.76	0.05	6.58
	2000	−27.39	0.02	−22.83	0.10	4.37	0.38	7.97

BGD
12, 2381–2427, 2015

Table 3. Mean (±SD) stable isotope values of the main groups of organisms sorted in the largest size fraction (> 2000 µm). *n* = number of samples analysed.

Groups	*n*	δ^{13}C (‰)	δ^{15}N (‰)
Salps	12	−22.36 ± 0.82	3.87 ± 1.29
Copepods	15	−21.98 ± 0.95	4.40 ± 0.54
Euphausiacea	12	−21.03 ± 2.34	4.24 ± 0.63
Amphipods	9	−23.19 ± 0.24	4.14 ± 0.41
Pteropods Gymnosoms	5	−23.44 ± 0.04	4.56 ± 0.09
Chaetognaths	12	−22.94 ± 0.18	5.93 ± 0.60
Polychaetes *Tomopteris*	3	−22.52 ± 0.03	7.72 ± 0.06
Fish larvae	3	−21.60 ± 0.05	5.99 ± 0.08

BGD
12, 2381–2427, 2015

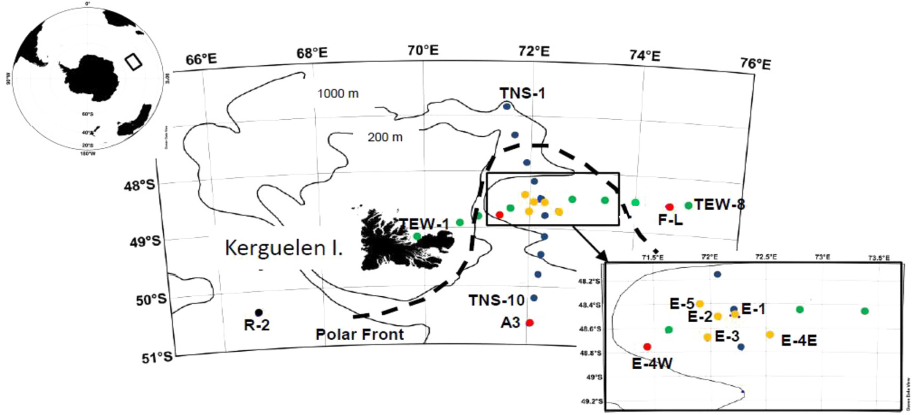

Figure 1. Map of the KEOPS2 study area. The locations of the stations are marked by color dots. Blue indicates the stations of the North–South transect (TNS), green indicates the stations of the East–West transect (TEW), orange indicates the stations E located in the meander of the polar front (zoom panel). Red stands for other stations located in the fertilized region and black stands for the station located in the HNLC region.

BGD
12, 2381–2427, 2015

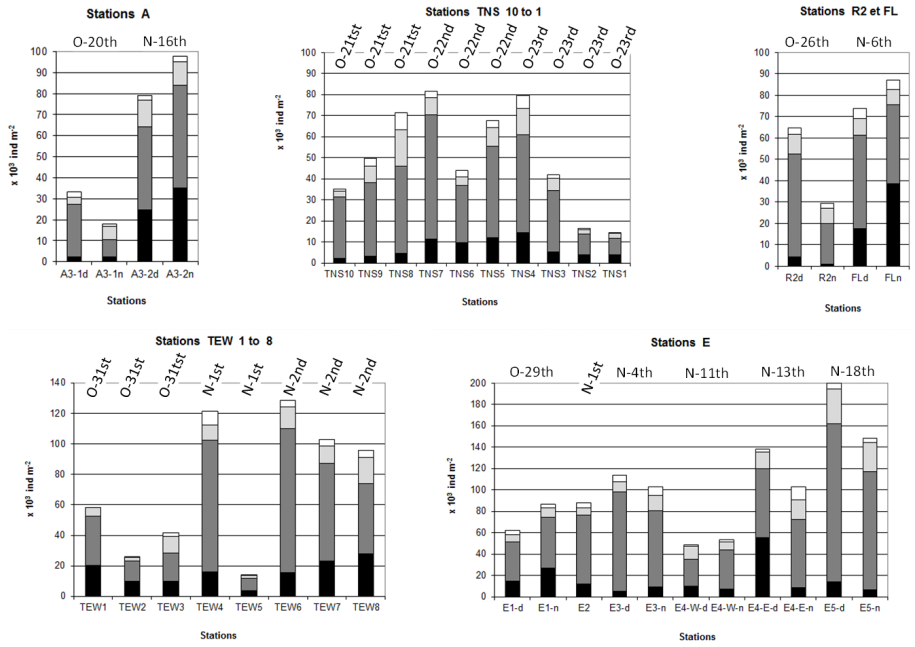

Figure 2. Integrated 0–250 m mesozooplankton abundance for the different stations sampled during KEOPS2 with size fractions distributions. Size fractions: < 500 µm: black; 500–1000 µm: dark gray; 1000–2000 µm: light gray; > 2000 µm: white.

BGD
12, 2381–2427, 2015

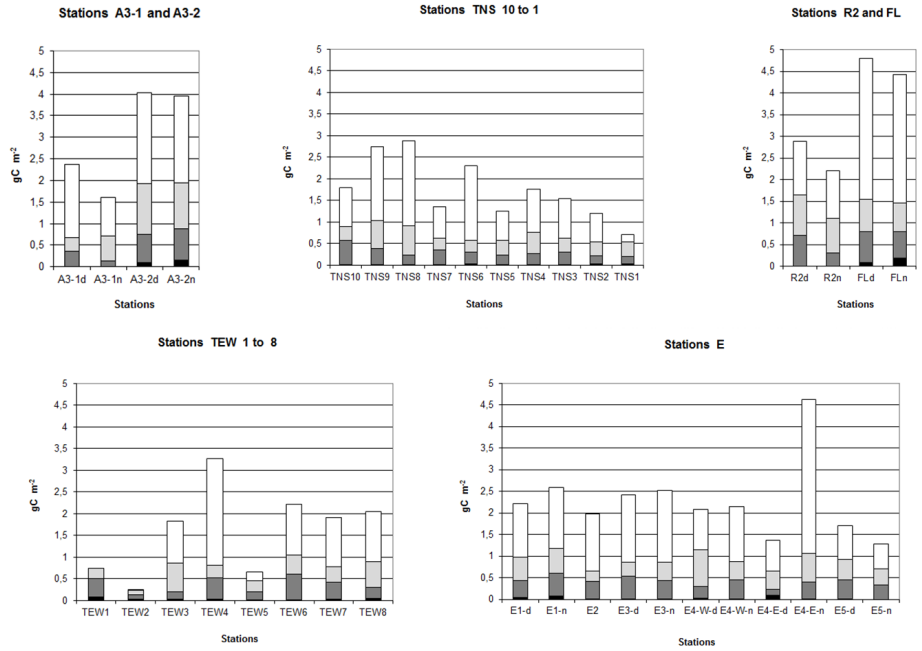

Figure 3. Integrated 0–250 m mesozooplankton biomass for the different stations sampled during KEOPS2 with size fractions distributions. Size fractions: < 500 µm: black; 500–1000 µm: dark gray; 1000–2000 µm: light gray; > 2000 µm: white.

BGD
12, 2381–2427, 2015

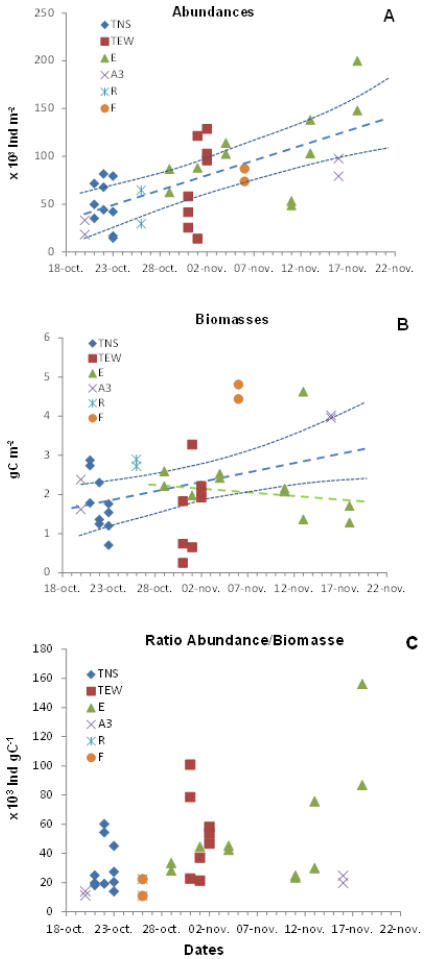

Figure 4. (a) Abundance and **(b)** biomasses values and **(c)** ratio abundance on biomasses for the different stations visited during KEOPS2 over sampling dates.

BGD
12, 2381–2427, 2015

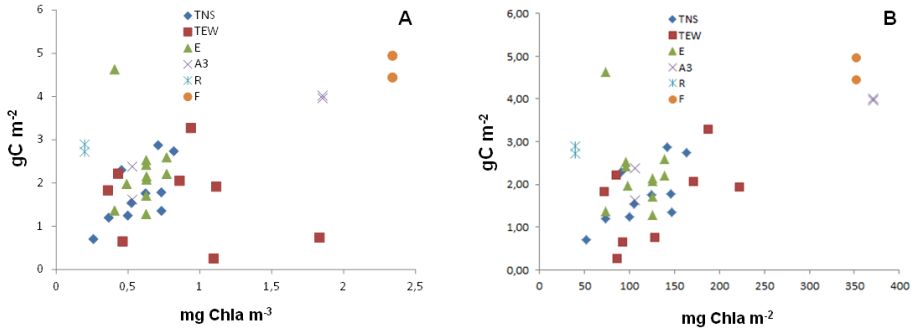

Figure 5. Zooplankton biomass values against average Chl *a* in the upper 100 m **(a)** and against the integrated Chl *a* in the mixed layer depth **(b)** for the different stations visited during KEOPS2.

BGD
12, 2381–2427, 2015

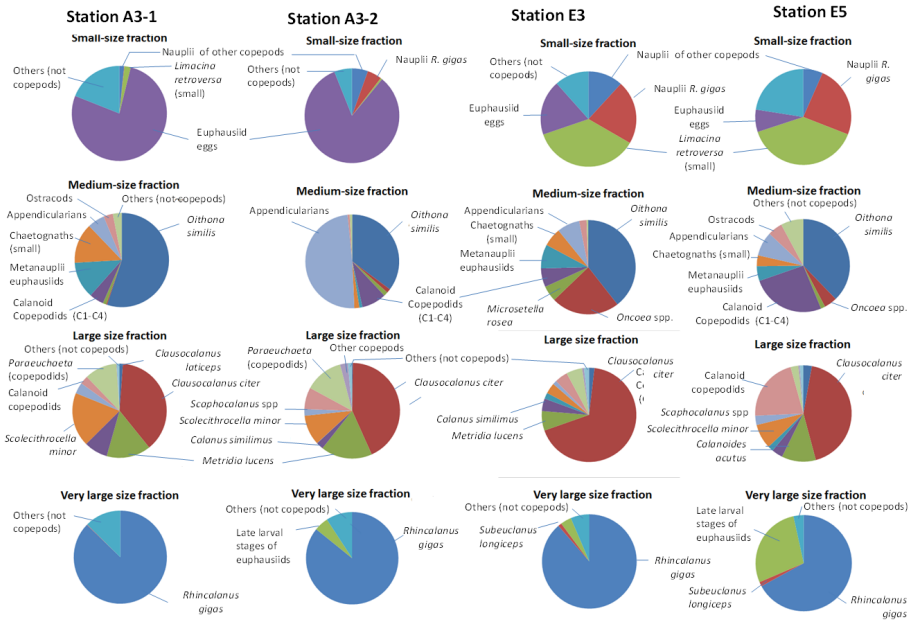

Figure 6. Distribution of main taxa abundances within each of the four size fractions. Average distributions between day and night samples at stations A3-1, A3-2, E3 and E5. For each size fraction, the color labels for the different taxa are similar.

BGD
12, 2381–2427, 2015

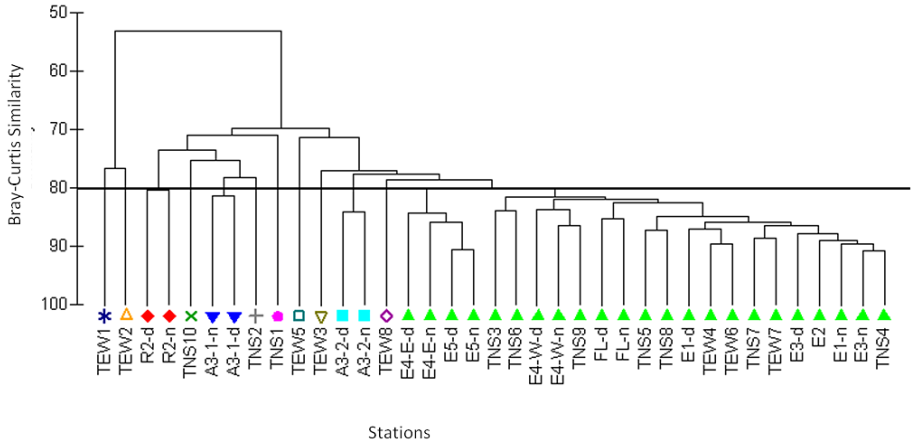

Figure 7. Dendrogram produced by the clustering of the 37 samples (28 stations, among them 9 stations with day-night sampling) during KEOPS2 based on the density (ind m^{-3}) of mesozooplankton taxa. Density values were fourth-root transformed prior to analysis of the Bray–Curtis similarity matrix.

BGD
12, 2381–2427, 2015

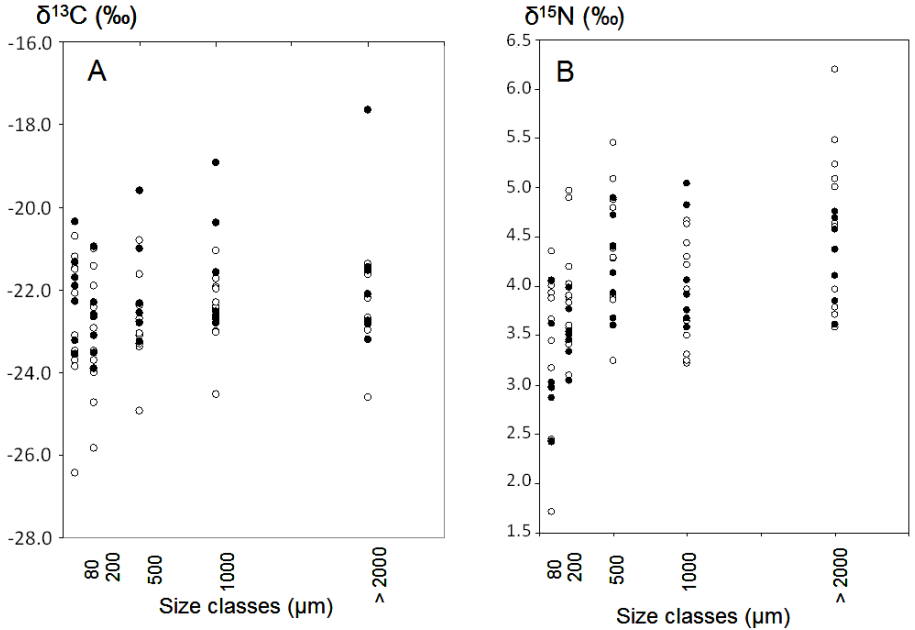

Figure 8. Distribution of $\delta^{13}C$ **(a)** and $\delta^{15}N$ **(b)** of zooplankton across size-fractions during KEOPS2. White symbols = day; Black symbols = night.

BGD
12, 2381–2427, 2015

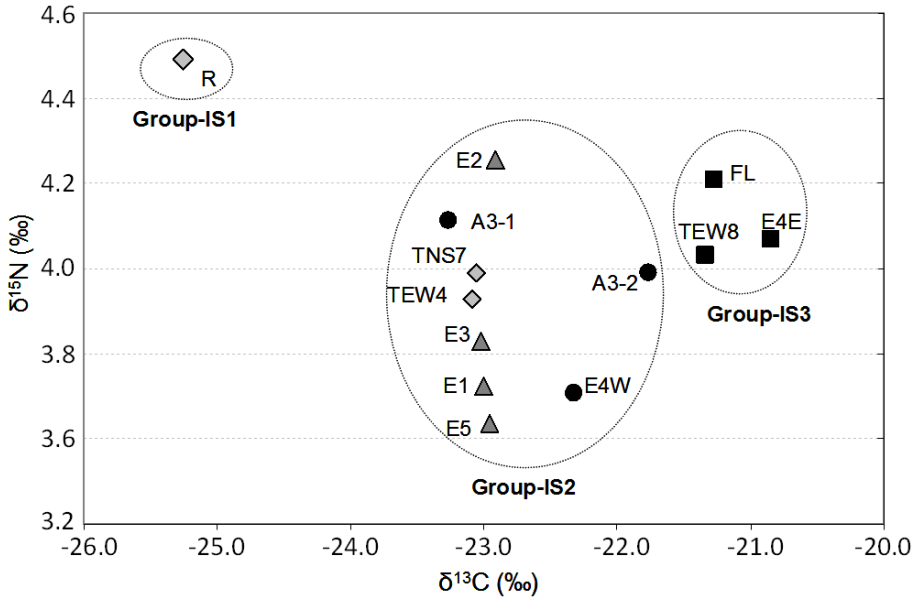

Figure 9. Mean $\delta^{13}C$ and $\delta^{15}N$ values of zooplankton for stations sampled during KEOPS2 cruise. Circles indicate the 3 isotopic groups (IS-Group 1, IS-Group 2, IS-Group 3) based on hierarchical analysis on stable isotope values. Symbols correspond to phytoplankton groups based on chemometric measurements (T-Groups) by Trull et al. (2015). Grey diamonds = T-Group 1; Dark grey triangles = T-Group 2; Black dots = T-Group 3; Black squares = T-Group 5.

BGD
12, 2381–2427, 2015

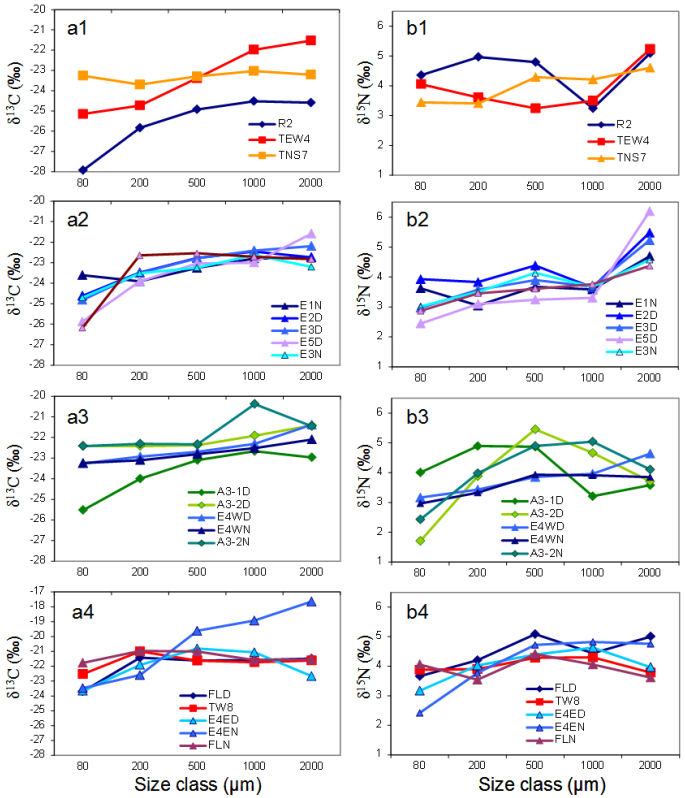

Figure 10. Distribution of δ^{13}C (left column, **a**) and δ^{15}N (right column, **b**) values across zooplankton size-fractions for 4 of the 5 T-Groups of stations used by Trull et al. (2015) for phytoplankton, except E4-E included here in T-Group 5 instead of T-Group 2. From top to bottom: A1 and B1 = T-Group 1, A2 and B2 = T-Group 2, A3 and B3 = T-Group 3, A4 and B4 = T-Group 5.

BGD
12, 2381–2427, 2015